DESIGN OF ROBUST LOW-ORDER CONTROLLERS FOR COMPLEX PROCESSES: A CASE STUDY ON REACTIVE DISTILLATION IN A MEDIUM-SCALE PILOT PLANT

Marten Völker * **Christian Sonntag** * **Sebastian Engell** *

* *Process Control Laboratory, Department of Biochemical and Chemical Engineering, Universität Dortmund* [1]

Abstract: This paper deals with robust low-order controller design for a medium-scale pilot reactive distillation column. In the first step, a linear model of the column which is identified from experiments is used to compute the attainable control performance. In this step, actuator limitations and model uncertainty resulting from a priori knowledge as well as confidence intervals provided by the identification procedure are considered. In the second step, the result of the optimal control performance computation is employed in a frequency response approximation scheme to generate a low-order controller. Finally, the synthesised controller is validated at the reactive distillation column.

Keywords: reactive distillation, control of complex processes, robust control, multiobjective control, controller reduction

1. INTRODUCTION

In recent years, integrated reactive separation processes have attracted considerable attention in both academic research and industrial applications. In this paper, the operation of a pilot plant scale reactive distillation column operated at the Universität Dortmund is studied. The process exhibits input multiplicities such that, when applying linear control, tight constraints must be adhered to in order to avoid sign changes of the process gains. To fulfil these constraints and to operate the plant efficiently, an examination of potential control approaches was performed. In previous work (Völker (2002)), a control structure was identified which provides good performance with respect to the rejection of disturbances. It was shown by simulation of a rigorous nonlinear plant model that linear control is possible in the vicinity of the nominal operating point which was determined by dynamic optimisation (Fernholz et al. (1999)). A controller that is implemented on the real pilot plant has to satisfy a set of constraints and design specifications such as minimising the control error while keeping bounds on actuator ranges and robust stability. These specifications are met here by using a two-step procedure: In the first step, a high-order multiobjective controller is designed which satisfies the specifications, while in a second step, low-order controllers are synthesized by an order reduction scheme such that the specifications are also met for the reduced controller. In the first step, we follow the lines of Boyd and Barrat (1991); Sznaier et al. (2000); Scherer (1995); Hindi et al. (1998) using finite dimensional Q-parametrisation where reduced conservatism is bought at the expense of computational complexity. In our approach, for increased flexibility, the optimisation is not performed in the state space but employing point-wise matrix descriptions in the time and in the frequency domain as described in Webers and Engell (1996b). The point-

[1] With financial support of the Deutsche Forschungsgemeinschaft to the research cluster ”Integrated Reaction and Separation Processes” (FOR 344)

wise approach requires some engineering judgement in choosing the gridding parameters, but, on the other hand, many different performance objectives such as e. g. actuator saturation, overshoot constraints, steady-state accuracy, and arbitrary trajectories of the external inputs etc. (see Webers and Engell (1996b,a); Webers (1997b)) can be handled. Furthermore, it is amenable to intrinsically point-wise constraint descriptions such as e. g. uncertainty bounds resulting from the asymptotic theory of identification (see e. g. Zhu (1989)) which renders it attractive from a practical point of view. For the design process in the case of the reactive distillation column, we use a model obtained by means of system identification. An unstructured uncertainty description of the model is calculated, combining the model invalidation method described in Poolla et al. (1994) and heuristic knowledge about the process behaviour. This uncertainty description is then used to set up a multiobjective performance optimisation in which, besides robustness, also process constraints such as actuator saturation are imposed. In a second step, a low-order controller is obtained by means of frequency response approximation (Engell (1988); Engell and Müller (1991); Engell and Pegel (2000)). It is shown that, in the case of the reactive distillation column, the reduced-order controller meets the original multiobjective specifications and, due to its low order, renders the control scheme practically applicable. The remainder of the paper is organised as follows. We first briefly review the performance optimisation approach. The second part is concerned with the controller reduction technique using frequency response approximation. The focus of this paper lies on the application to the reactive distillation column which is described in the third part.
Our notation is that all possibly multivariate variables are printed in bold font. We use the Matlab-like notation $\mathbf{X}(:,j)$ to denote subparts of matrices, in this case the subpart is the jth column of the matrix $\mathbf{X}$. In the course of the paper, frequent use will be made of the following operators which can be applied to frequency- or time-dependent matrices ($\mathbf{X}(j\omega), \mathbf{X}(t)$), as well as transfer matrices ($\mathbf{X}(s)$):

- transpose ^{T},
- complex conjugate transpose ^{H},
- stacking operator col, where

$$col(\mathbf{X}) := [X_{11}, X_{21}, \ldots, X_{m1}, X_{12}, \ldots, X_{1n}, \ldots, X_{mn}]^T, \tag{1}$$

- Kronecker operator $\otimes$, where

$$\mathbf{X} \otimes \mathbf{Y} := \begin{bmatrix} X_{11} \cdot \mathbf{Y} & X_{12} \cdot \mathbf{Y} & \ldots & X_{1n} \cdot \mathbf{Y} \\ X_{21} \cdot \mathbf{Y} & \ddots & & \vdots \\ \vdots & & \ddots & \vdots \\ X_{m1} \cdot \mathbf{Y} & & & X_{mn} \cdot \mathbf{Y} \end{bmatrix}. \tag{2}$$

2. COMPUTATION OF THE OPTIMAL CONTROL PERFORMANCE

2.1 Multiobjective Specifications

The interaction of a linear time invariant plant with a controller $\mathbf{K}(s)$ and the relation of the external inputs $\mathbf{w}$ to the external outputs $\mathbf{z}$ are described by introducing a generalised plant $\mathbf{P}(s)$ which is shown in Fig. 1. Here, $\mathbf{u}$ denotes the outputs of the controller, and $\mathbf{v}$ denotes the inputs of the controller. The relationship between $\mathbf{w}$ and $\mathbf{z}$, including the controller,

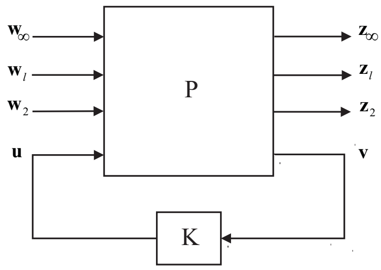

Fig. 1. Generalised plant configuration for multiobjective performance calculation.

is then given by the linear fractional transformation $\mathbf{T}_{zw} := \mathbf{P}_{11} + \mathbf{P}_{12}\mathbf{K}(\mathbf{I} - \mathbf{P}_{22}\mathbf{K})^{-1}\mathbf{P}_{21}$. We consider three different types of performance specifications:

- $\mathbf{w}_2, \mathbf{z}_2$: This performance channel is used in the objective function. Several different objectives can be combined. We will formulate a finite horizon integral squared error problem in the time domain
$$\|\mathbf{T}_{z_2 w_2}\|_{2,\mathbf{t}} := \int_0^{t_{n_t}} foh\left\{\mathbf{z}_2^T(t)\mathbf{z}_2(t)\right\} dt, \tag{3}$$
where foh denotes first order hold approximation and $\mathbf{w}_2$ is specified a priori.
- $\mathbf{w}_l, \mathbf{z}_l$: This channel is used to impose limitations
$$\max|\mathbf{z}_l(t)| < \gamma_l \; \forall \; t \in \mathbf{t}_{spec}, \tag{4}$$
with respect to a set of predefined signals $\mathbf{w}_l$ and an arbitrary time window $\mathbf{t}_{spec}$. These constraints include steady-state accuracy, actuator saturation avoidance (e. g. in an impulse-to-peak sense), constraints on the maximum overshoot, just to mention a few (see Webers and Engell (1996b) for more details).
- $\mathbf{w}_\infty, \mathbf{z}_\infty$: This channel is used to enforce robustness constraints of the form
$$\max_{\omega \in \mathbf{\Omega}} \|\mathbf{T}_{\mathbf{z}_\infty \mathbf{w}_\infty}(j\omega)\mathbf{l}_\Delta(j\omega)\|_{i2} < \gamma_\infty, \tag{5}$$
where $\mathbf{\Omega}$ is a set of frequency points, $_{i2}$ denotes the induced 2-norm and $\mathbf{l}_\Delta$ is an uncertainty weighting matrix.

2.2 Finite Dimensional Q-Parametrisation

Using the well-known Youla parametrisation (Youla et al. (1976)), any relationship between the external signals $\mathbf{w}(s)$ and the external outputs $\mathbf{z}(s)$ which is attainable by a stabilising controller can be described as

$$\mathbf{T}_{zw}(s) = \mathbf{T}_{11}(s) + \mathbf{T}_{12}(s) \cdot \mathbf{Q}(s) \cdot \mathbf{T}_{21}(s), \quad (6)$$

for some $\mathbf{Q} \in \mathcal{H}_\infty$; all such $\mathbf{Q}$ yield an internally stable closed-loop system. Eq. (6) is a complete and convex description of all possible closed-loop systems. To compute the optimal control performance, the Youla parameter $\mathbf{Q}(s)$ must be parameterised by a finite number of parameters. The usual approach is to represent $\mathbf{Q}$ by a finite series in terms of suitable fixed transfer matrices $q_i(s)$ and variable coefficients x_i. In the general multivariate case, a finite dimensional $\tilde{\mathbf{Q}}$ can be written as

$$col(\tilde{\mathbf{Q}}(s, \mathbf{x})) := \mathbf{I}_{n_v n_u} \otimes \mathbf{q}^T(s) \cdot \mathbf{x}, \quad (7)$$

with

$$\mathbf{q}^T(s) := [q_0(s) \ldots q_{n_b-1}(s)] \quad (8)$$

as any appropriate basis of $\mathcal{H}_\infty$ for $n_b \to \infty$.

2.3 Finite Horizon and Gridding

The closed-loop relationship (6) can be reformulated to avoid time consuming computations during the optimisation (Webers (1997a)). In the frequency domain, the closed-loop relationship (6) is evaluated point-wise as an affine function of the optimisation vector $\mathbf{x}$:

$$col(\mathbf{T}_{zw}(j\omega, \mathbf{x})) = \mathbf{T}_A(j\omega) + \mathbf{T}_B(j\omega) \cdot \mathbf{x}, \\ \omega \in \mathbf{\Omega} = [\omega_1 \ldots \omega_{n_\omega}]. \quad (9)$$

In the time domain, the reaction of the closed loop to the jth external input w_j is given as an affine function of the optimisation vector $\mathbf{x}$ by:

$$\mathbf{z}_{w_j}(t, \mathbf{x}) = \tilde{\mathbf{T}}_{A:w_j}(t) + \tilde{\mathbf{T}}_{B:w_j}(t) \cdot \mathbf{x}, \\ t \in \mathbf{t} = [t_1 \ldots t_{n_t}]. \quad (10)$$

Eqs. (9) and (10) give a complete and affine description of all possible closed-loop systems with respect to the optimisation vector $\mathbf{x}$.

2.4 Formulation as an Optimisation Problem

Using the point-wise description (10), the integral squared error objective (3) is mapped to a quadratic optimisation problem (Pegel and Engell (2000)):

$$\min_{\mathbf{x}} \underbrace{\frac{1}{2} \cdot \mathbf{x}^T \cdot \mathbf{H} \cdot \mathbf{x} + \mathbf{c}^T \cdot \mathbf{x}}_{:=\mathbf{\Phi}(\mathbf{x})}. \quad (11)$$

The constraints (4) are mapped to a set of linear constraints:

$$\mathbf{A} \cdot \mathbf{x} \leq \mathbf{b}. \quad (12)$$

The constraints (5) are evaluated by a new method of solving a sequence of optimisation problems (11), see Völker and Engell (2004, 2005). Since the multiobjective performance calculation described above is based on a finite dimensional Q-parametrisation, it usually yields high-order controllers which leads to the necessity of controller reduction.

3. FREQUENCY RESPONSE APPROXIMATION

The main idea of the frequency response approximation scheme is that the closed loop containing the low-order controller should behave like the closed loop containing the high-order controller. It was shown in Engell (1988) that this goal can be adequately addressed if the difference between the closed loops is described by the Frobenius norm of its frequency response. For simple controllers, this leads to the minimisation of a convex optimisation functional where stability of the approximated loop can be formulated as an optimisation constraint. Let $\mathbf{T}_0(j\omega)$ be the frequency response of the ideal complementary sensitivity function resulting from the control performance optimisation corresponding to a high-order controller $\mathbf{K}_0(j\omega)$ [2], not necessarily the one presented in this paper. Let $\mathbf{G}(j\omega)$ and $\mathbf{K}(j\omega)$ denote the frequency responses of the plant and the approximated controller. Then it follows from straightforward manipulations that the difference between the approximated complementary sensitivity $\mathbf{T}$ and the ideal $\mathbf{T}_0$, where we for clarity omit the frequency argument $(j\omega)$ from here on, satisfies:

$$\begin{aligned} \mathbf{\Delta_T} : &= \mathbf{GK}(\mathbf{I} + \mathbf{GK})^{-1} - \mathbf{T}_0 \\ &= \mathbf{S}[\mathbf{GK} - \mathbf{GK}_0]\mathbf{S}_0 \\ &= \mathbf{SG}\Delta_\mathbf{K}\mathbf{S}_0, \end{aligned} \quad (13)$$

where we have additionally used the sensitivity functions, $\mathbf{S}_0$ and $\mathbf{S}$, which fulfil $\mathbf{S}_0 + \mathbf{T}_0 = \mathbf{S} + \mathbf{T} = \mathbf{I}$. In contrast to Engell and Müller (1991), no exact minimisation of $\|\mathbf{\Delta_T}\|_{Fro}$ is performed. Instead, we approximate $\mathbf{S} \approx \mathbf{S}_0$ which is reasonable if the reduced-order controller achieves $\mathbf{T} \approx \mathbf{T}_0 \Leftrightarrow \mathbf{S} \approx \mathbf{S}_0$. Then, (13) becomes affine in $\mathbf{K}$. If $\mathbf{K}$ is chosen to be affine in an optimisation parameter $\mathbf{x}$, e. g. by

$$col(\mathbf{K}) := \mathbf{I}_{n_v \cdot n_u} \otimes \underbrace{[k_1(s) \ldots k_n(s)]}_{:=\mathbf{k}^T} \cdot \mathbf{x}, \quad (14)$$

the Frobenius norm of the approximation error can be written as:

$$\begin{aligned} \|\mathbf{\Delta}_T\|_{Fro}^2 &= \|\mathbf{W}_u \cdot \mathbf{\Delta}_K \cdot \mathbf{W}_y\|_{Fro}^2, \\ &= \|col(\mathbf{W}_u\mathbf{K}\mathbf{W}_y) - col(\mathbf{W}_u\mathbf{K}_0\mathbf{W}_y)\|^2 \\ &= \| \underbrace{\mathbf{W}_y^T \otimes \mathbf{W}_u \cdot \mathbf{I}_{n_y \cdot n_u} \otimes \mathbf{k}^T}_{:=\mathbf{A}} \cdot \mathbf{x} \\ &\quad - \underbrace{\mathbf{W}_y^T \otimes \mathbf{W}_u \cdot col(\mathbf{K}_0)}_{:=\mathbf{B}} \|^2 \end{aligned}$$

[2] We recover $\mathbf{K}_0$ from a linear fractional transformation of the stabilising Youla observer and $\mathbf{Q}$ (see e. g. Zhou (1998)).

$$= \mathbf{x}^T \mathbf{A}^H \mathbf{A}\mathbf{x} - 2\mathbf{B}^H \mathbf{A}\mathbf{x} + \mathbf{B}^H \mathbf{B}$$
$$= \mathbf{x}^T \Re\{\mathbf{A}^H \mathbf{A}\}\mathbf{x} - 2\Re\{\mathbf{B}^H \mathbf{A}\}\mathbf{x} + \Re\{\mathbf{B}^H \mathbf{B}\}, \tag{15}$$

where $\mathbf{W}_u := \mathbf{S}_0\mathbf{G}$ and $\mathbf{W}_y := \mathbf{S}_0$. This can be cast as a quadratic optimisation problem (11), and the condition for nominal stability of the closed loop with the approximated controller given by Enns (1984):

$$\|\mathbf{S}_0 \mathbf{G} \mathbf{\Delta}_K\|_{i2} < 1, \tag{16}$$

can be considered by the iterative technique proposed in Völker and Engell (2005).

4. APPLICATION TO THE REACTIVE DISTILLATION COLUMN

4.1 The Reactive Distillation Column

In this paper, the heterogeneously catalysed esterification of acetic acid and methanol to methyl acetate and water in a pilot plant operated at the Department of Biochemical and Chemical Engineering in Dortmund is studied. The pilot plant is 9 meters high and has a diameter of 100 millimeters. A scheme of the plant is depicted in Fig. 2. It consists of three parts, the reboiler, the condenser and reflux, and the column itself. Within the column, there are three sections of structured packings, two catalytic ones at the bottom and a separating section at the top of the column. Each packing has a length of 1 meter. The plant is operated

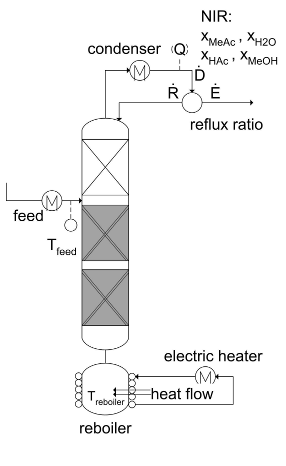

Fig. 2. Scheme of the semibatch reactive distillation column.

in semi-batch mode. This means that, in a first step, the reboiler is filled with methanol which is then evaporated. After gaseous methanol has ascended within the column body, the acetic acid feed is opened until the concentration of methanol is too low to achieve the desired product concentration. The essential degrees of freedom are the reflux ratio [3], the acetic acid feed (feed) and the heat flow supplied to the reboiler via an electrically heated water pipe system. These degrees of freedom were used to obtain an efficient nominal operating point by means of nonlinear optimisation of the productivity using a rigorous nonlinear model (Fernholz et al. (1999)). During the optimisation, constraints ensuring a minimum conversion of acetic acid were added.

4.2 Control Structure Selection

Due to the semi-batch mode of operation, the process does not reach a steady state. For the investigation of the process operability, the quasi-stationary process gains were investigated. To this end, the reaction of potential controlled variables at the end of reasonably long periods where the degrees of freedom were held constant was analysed using a rigorous nonlinear process model. These quasi-stationary diagrams showed that the process exhibits multiple changes of sign with respect to the manipulated variables reflux ratio and acetic acid feed and the heat flow to the reboiler. As was shown in several rigorous simulation studies during which the robustness against typical uncertainty scenarios was checked (see Fernholz et al. (1999); Völker (2002); Sonntag (2004)), the process model can be controlled efficiently at its nominal operating point by a linear control law, if a control structure is chosen that employs as controlled variables (CVs) the liquid phase compositions in the reflux $\mathrm{x}_{\mathrm{MeAc}} \left[\frac{\mathrm{mole}}{\mathrm{mole}}\right]$ and $\mathrm{x}_{\mathrm{H_2O}} \left[\frac{\mathrm{mole}}{\mathrm{mole}}\right]$ which are measured online by near-infrared (NIR) spectroscopy. In Völker (2002), optimal linear control performance calculation, rigorous nonlinear simulation, and a priori process knowledge were used to corroborate these results [4]. For this control structure, the next step was to design a robust linear controller for the nonlinear mapping $\mathcal{G}$:

$$\begin{bmatrix} y_1(\mathrm{x}_{\mathrm{MeAc}}) \\ y_2(\mathrm{x}_{\mathrm{H_2O}}) \end{bmatrix} = \mathcal{G}\left(\begin{bmatrix} u_1(\text{reflux ratio}) \\ u_2(\text{feed}) \end{bmatrix} \right), \tag{17}$$

based on an identified linear model and a description of model uncertainties that remained due to the nonlinear and time-varying process behaviour.

4.3 Identification for Control of a Linear Process Model

On 2004-09-09, an identification experiment was conducted at the real plant during which the process was excited with generalised binary noise signals (see Tulleken (1990)) in an identification region depicted by the gray surfaces in Fig. 3. This figure shows the quasi-stationary behaviour of the controlled variables as a function of the reflux ratio and the feed recorded by simulation of the nonlinear model. A slightly suboptimal operating point, as indicated by the crosses in Fig. 3, was chosen to reduce the risk of gain changes, while the nominally optimal operating conditions were maintained approximately. After the com-

[3] Here defined as the ratio $\frac{\dot{R}}{\dot{D}}$ in the interval $[0, 1]$, see Fig. 2.

[4] The general methodology was e. g. presented in Engell et al. (2004).

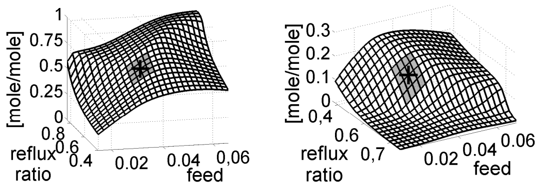

(a) x_{MeAc} (b) $x_{\mathrm{H_2O}}$

Fig. 3. Stationary characteristic diagrams of the CVs (heat flow = 3.667 kW).

pensation of time delays, the mean value of the data sets was removed. Scaling of the data was performed according to $\mathbf{y}_s = \mathbf{L}\mathbf{y}$ and $\mathbf{u}_s = \mathbf{R}^{-1}\mathbf{u}$, where the input scaling matrix $\mathbf{R}$ was chosen to represent the identification excitation while the output scaling matrix $\mathbf{L}$ represents the control goal. The matrices are given by:

$$\mathbf{L} = \begin{pmatrix} \frac{1}{0.06} & 0 \\ 0 & \frac{1}{0.03} \end{pmatrix}, \quad \mathbf{R} = \begin{pmatrix} 0.05 & 0 \\ 0 & 0.005 \end{pmatrix}. \qquad (18)$$

In order to reduce the effect of slow drifts on the estimated model, the input and output data was highpass-filtered using a fourth-order lead element G_F given by $G_F = \left(\frac{s+3.162\cdot10^{-5}}{s+3.162\cdot10^{-4}}\right)^4$, which provides a stop-band attenuation of 80 dB. Model estimation was performed employing an estimation algorithm based on orthonormal basis functions (Van Den Hof et al. (1995)). The order of the estimated model was determined using the Final Output Error criterion described in Zhu (2001). Since the estimated model is of high order, model reduction using frequency response approximation was employed. In this step, in order to emphasise the estimated crossover frequency of the closed loop (roughly at $10^{-3}\ \frac{rad}{sec}$), a weight $G_W(s) = 0.005\frac{s+1.581\cdot10^{-4}}{(s+0.005)(s+1.581\cdot10^{-3})}$, was used which represents a lead element in series with a first-order delay element.

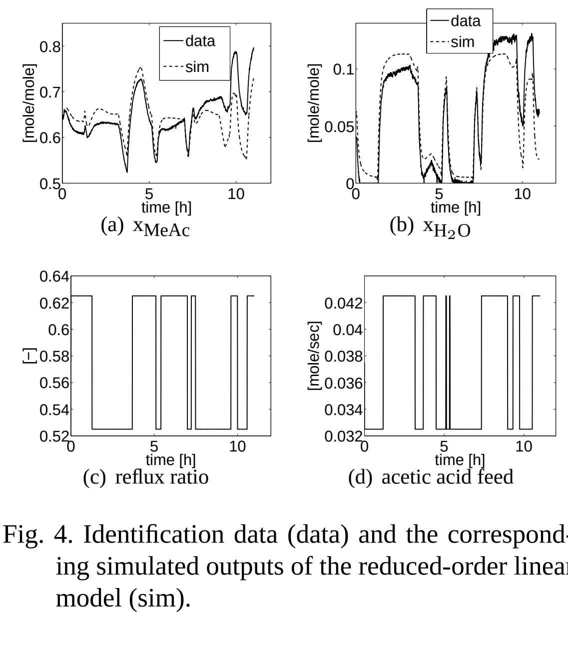

(a) x_{MeAc} (b) $x_{\mathrm{H_2O}}$ (c) reflux ratio (d) acetic acid feed

Fig. 4. Identification data (data) and the corresponding simulated outputs of the reduced-order linear model (sim).

Fig. 4 depicts a comparison of the identification data and the outputs of the estimated (unscaled) model into which, for simulation purposes, the estimated time delay was incorporated using a standard zero-order-hold transform of Pade's approximation. The continuous-time version of the corresponding transfer function of the identified system (time unit is seconds) mapping changes in the reflux ratio and the acetic acid feed to changes in the mole fractions x_{MeAc} and $x_{\mathrm{H_2O}}$ around the nominal operating point is given by:

$$\begin{aligned}
G_{11}(s) &= \\
&-0.0026\frac{(s-0.0105)(s-6.73\cdot10^{-6})}{(s+0.0118)(s+0.0025)(s+4.46\cdot10^{-5})} \\
G_{12}(s) &= \\
&-0.0070\frac{(s-0.0105)(s+0.0012)}{(s+0.0118)(s^2+0.0010s+8.28\cdot10^{-7})} \\
G_{21}(s) &= \\
&0.0011\frac{(s+0.0483)(s-0.0105)}{(s+0.0188)(s+0.0118)(s+0.0030)} \\
G_{22}(s) &= \\
&-0.0011\frac{(s-0.0105)(s+0.0012)}{(s+0.0118)(s^2+0.0011s+5.39\cdot10^{-7})}
\end{aligned} \qquad (19)$$

Fig. 4 shows that the time-varying and nonlinear process cannot be completely represented by the linear model. Hence, plant-model mismatch must be accounted for when designing the controller. To this end, an invalidation scheme (see Poolla et al. (1994)) was used to derive robustness bounds using the identification data set. In this approach, also potential nonlinearities are considered. Since the identified time delay can also vary due to fluctuations in the heat flow, and it is not possible to identify it with high accuracy from the data set, we used the formula given by Lundström (1994) to account for uncertain time delays of up to 170 sec. The output-multiplicative uncertainty weight $\mathbf{l}_\Delta$ ($\|\mathbf{\Delta}\|_{i2} < 1$) resulting from the superposition of invalidation and time delay boundaries is shown in Fig. 5.

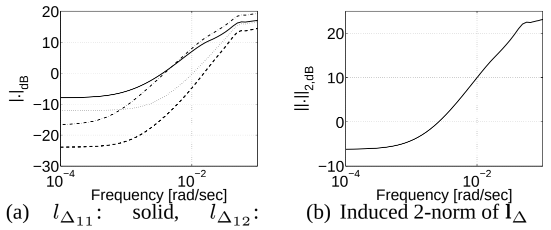

(a) $l_{\Delta_{11}}$: solid, $l_{\Delta_{12}}$: dashed, $l_{\Delta_{21}}$: dotted, $l_{\Delta_{22}}$: dash-dotted (b) Induced 2-norm of $\mathbf{l}_\Delta$

Fig. 5. Output-multiplicative uncertainty as a result of the identification scheme.

4.4 Control Performance Calculation

For the optimisation, we used the generalised plant setup as depicted in Fig. 6, where we employed the transfer function scaled according to (18). In the objective function, the integral squared control error $e(t)$ to unit steps in the setpoints $r(t)$ is considered. Since we end up with Hessian matrices for each reference-control-error pair which can be superimposed in the optimisation, it is possible to weight the coupling, i. e. the reaction of e_j to r_i for $i \neq j$ less than setpoint tracking ($i = j$). In the context of the reactive distillation column example, the weighting of the coupling was smaller than that of the setpoint tracking by a factor of 2, since disturbance rejection rather than decoupled setpoint tracking was desired. The uncertainties (see Fig. 5) were given in output-multiplicative form such that, with $\mathbf{T}_{z_\infty w_\infty}$ being equal to the negative setpoint-to-output complementary sensitivity ($r \to y$, Fig. 6), the condition for robust stability is given by:

$$\|\mathbf{T}_{z_\infty w_\infty}(j\omega)\mathbf{l}_\Delta(j\omega)\|_{i2} < 1 \; \forall \omega \in \mathbf{\Omega}. \tag{20}$$

We also imposed actuator saturation constraints on the manipulated variables, i. e. we specified

$$|\mathbf{z}_l(t)| < \gamma_l \quad \forall t \in \mathbf{t}_l = \mathbf{t}, \tag{21}$$

where $\mathbf{z}_l = \mathbf{u}$ in Fig. 6 and $\gamma_l = 2$. The multiobjective performance computation parameters are summarised in Tab. 1.

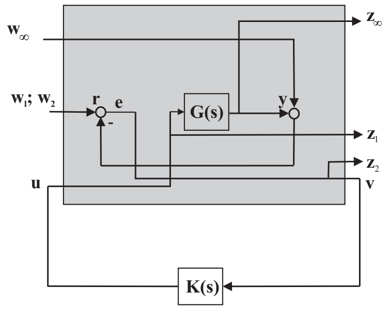

Fig. 6. Generalised plant for multiobjective design.

basis functions
$\mathbf{q}^T = \left[\frac{1}{s+\epsilon}\; 1 \; \frac{\omega_1}{s+\omega_1} \cdots \frac{\omega_{n_b-1}}{s+\omega_{n_b-2}}\right]$
$\omega_1 = 10^{-6}; \omega_{n_b-2} = 0.1; n_b = 16$
time discretisation
$\mathbf{t} = [t_1 \ldots t_{n_t}]$
$t_1 = 0; t_{n_t} = 30000; n_t = 3001$
frequency discretisation
$\mathbf{\Omega} = [\omega_1 \ldots \omega_{n_\omega}]$
$\omega_1 = 10^{-4}; \omega_{n_\omega} = 0.1; n_\omega = 50$
symmetric actuator saturation
$\|\mathbf{u}\|_{max} <= 2 \,\forall\, t \in \mathbf{t}_l = \mathbf{t})$

Table 1. Parameters used in the computation of the optimal control performance

The resulting controller $\mathbf{K}_0$ is of 72nd order. This controller was subsequently used in the frequency response approximation scheme outlined in section 3. The final unscaled reduced-order PI-controller is given by:

$$\mathbf{K}(s) = \begin{pmatrix} 0.2168\dfrac{(s+0.0015)}{s} & -0.9493\dfrac{(s+0.0016)}{s} \\ 0.1223\dfrac{(s+0.0010)}{s} & -0.0058\dfrac{(s+0.0013)}{s} \end{pmatrix}. \tag{22}$$

The comparison of the high- and low-order controllers on a setpoint step scenario for the identified linear model is depicted in Fig. 7. It can be seen in Figs. 7 and 8 that the reduced-order controller also satisfies the robustness constraint, the actuator saturation constraint, and that its nominal performance is similar to that of the high-order controller.

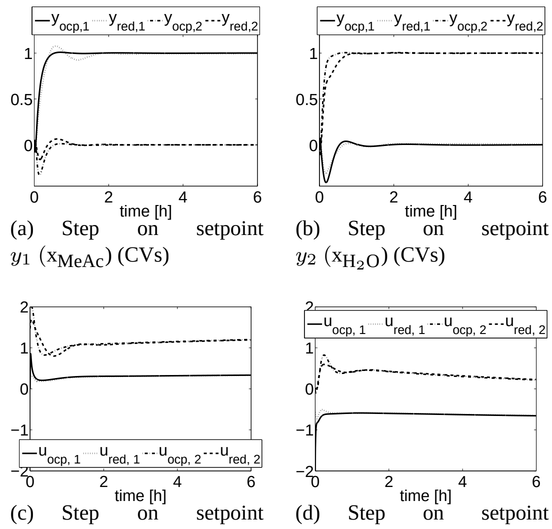

(a) Step on setpoint y_1 (x_{MeAc}) (CVs)

(b) Step on setpoint y_2 (x_{H_2O}) (CVs)

(c) Step on setpoint y_1 (x_{MeAc}) (MVs)

(d) Step on setpoint y_2 (x_{H_2O}) (MVs)

Fig. 7. Closed-loop step responses with optimal control performance controller (ocp) and reduced-order PI controller (red), all variables scaled according to (18).

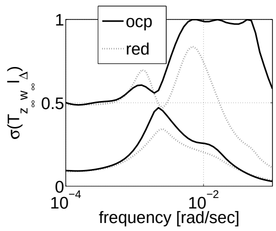

Fig. 8. Robustness constraints with optimal control performance controller (ocp) and reduced-order PI controller (red).

4.5 *Controller Validation at the Pilot Plant*

The reduced-order controller was implemented at the real experimental plant and tested in a setpoint change and disturbance scenario. Fig. 9 shows the main variables of the disturbance scenario. When the controller was activated after 2.15 hours, it could settle until, after 3.2 hours, a setpoint change was applied to drive the process to a more efficient mode of operation (see

Fig. 3). After 4.4 hours, the heat flow to the reboiler was increased to about 4.8 kW using a simple auxiliary control loop which controls the heat flow using an electrical heating system (see Fig. 9 (f)). This increase in the heat flow represents a large disturbance to nominal process operation. Finally, after 6.8 hours, the feed temperature was decreased by switching off the corresponding heating facility (Fig. 9 (g)). The reduced-order controller is capable of coping with the setpoint change and the large increase in the heat flow while it can not completely compensate the disturbance in the feed temperature. This can be attributed to the lack of methanol in the reboiler towards the end of a batch run (see Figs. 9 (e), (f), and (h)) which cannot be completely counteracted by the reduction of the acetic acid feed flow. After 10.5 hours, the controller had to be switched off due to depletion of the methanol supply in the reboiler.

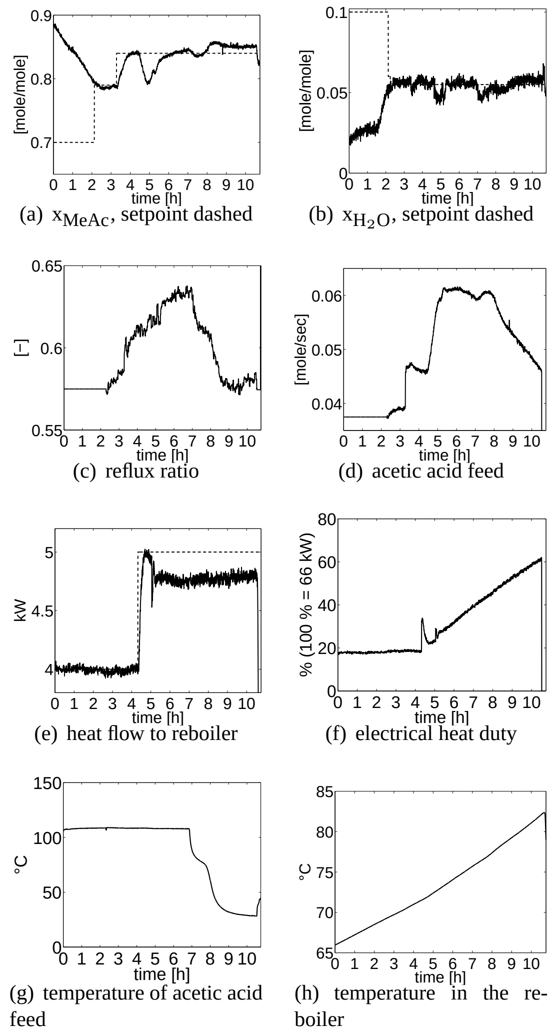

(a) x_{MeAc}, setpoint dashed (b) $x_{\mathrm{H_2O}}$, setpoint dashed

(c) reflux ratio (d) acetic acid feed

(e) heat flow to reboiler (f) electrical heat duty

(g) temperature of acetic acid feed (h) temperature in the reboiler

Fig. 9. Experimental results in a setpoint and disturbance rejection scenario.

On 2004/10/06, the same controller was tested in a pure setpoint scenario. As can be seen in Fig. 10, the controller is able to track the setpoints despite the pronounced nonlinearity of the plant.

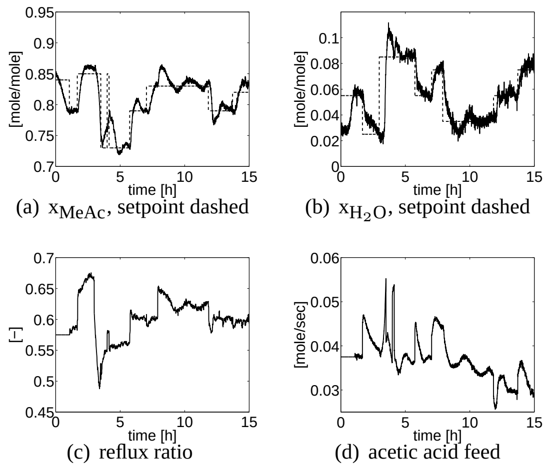

(a) x_{MeAc}, setpoint dashed (b) $x_{\mathrm{H_2O}}$, setpoint dashed

(c) reflux ratio (d) acetic acid feed

Fig. 10. Experimental results in a pure setpoint scenario.

5. CONCLUSION

We have shown how to design a multiobjective linear high-order controller by means of finite dimensional Q-parametrisation and the point-wise evaluation of the objective function as well as the constraints for the example of a reactive distillation column. The flexibility offered by this approach facilitates the consideration of practical objectives such as e. g. actuator saturation, especially when there are reasons to evaluate such criteria only on a finite horizon as is mandatory for the presented example, because the batch characteristics of the process can not be removed completely by filtering and model reduction. Additionally, the approach was used to handle the issue of robust stability. Generally, in our approach, the only source of conservatism is introduced by the finite dimensional Q-parametrisation which can be traded off against high controller orders. The controller order is not a problem, since we used the optimal high-order controller as a specification for designing a low-order controller which also fulfils the robust stability and actuator saturation specifications and only leads to a slight increase of coupling in the controlled variables. Finally, the controller was validated on the experimental plant twice. Both experiments showed that the controller performs well, for large setpoint changes and in the face of process disturbances which in open-loop operation would have driven the process far away from its specified operating regime. In future work, the setpoint scenario data presented in Fig. 10 will be used for closed-loop identification.

6. ACKNOWLEDGEMENTS

The support by the Deutsche Forschungsgemeinschaft (DFG) by funding of the research cluster FOR 344, ”Integrated Reaction and Separation Processes”, is gratefully acknowledged. We would like to thank our colleagues from the Chair of Fluid Separation Processes for the fruitful cooperation in the field of reactive distillation. Special thanks to Dirk Lieftucht, Queens University Belfast, for his support during major technical changes at the plant, and to the technicians of our laboratory.

REFERENCES

S. P. Boyd and C. Barrat. *Linear Controller Design: Limits of Performance.* Prentice Hall, Englewood Cliffs, 1991.

S. Engell. Compensator Design by Frequency-Weighted Approximation. *Proceedings of the IEE International Conference on Control*, pages 253–258, 1988.

S. Engell and R. Müller. Controller Design by Frequency-weighted Approximation: the Multivariable Case. In *IEE International Conference CONTROL-91*, pages 581–586, Edinburgh, 1991.

S. Engell and S. Pegel. Design of PID Controllers via Frequency Response Approximation. In *IFAC Workshop on Digital Control*, pages 65–72, Terrassa, Spain, 5-7.4. 2000.

S. Engell, J. O. Trierweiler, M. Völker, and S. Pegel. Tools and indices for dynamic controllability assessment and control structure selection. In *CACE Special Book: Integration of Design and Control*, pages 430–464. Elsevier, 2004. ISBN 0-444-51557-7.

D. F. Enns. *Model Reduction for Control Systems Design*. PhD Thesis, Stanford University, 1984.

G. Fernholz, S. Engell, and K. Fougner. Dynamics and Control of a Semibatch Reactive Distillation Process. In *2nd European Congress on Chemical Engineering*, Montpellier, Frankreich, 5.-7. Okt. 1999.

H. A. Hindi, B. Hassibi, and S. P. Boyd. Multiobjective $\mathcal{H}_2/\mathcal{H}_\infty$-Optimal Control via Finite Dimensional Q-Parametrization and Linear Matrix Inequalities. In *Proceedings of the American Control Conference*, pages 3244–3249, 1998.

P. Lundström. *Studies on Robust Multivariable Distillation Control*. PhD thesis, Norwegian University of Science and Technology, Trondheim, 1994.

S. Pegel and S. Engell. Computation of Achievable Performance of a Heat Integrated Distillation Column. In *Proceedings IFAC Conference on Control Systems Design*, pages 33–38, 2000.

K. Poolla, P. Khargonekar, A. Tikku, J. Krause, and K. Nagpal. A Time-domain Approach to Model Validation. *IEEE Transactions on Automatic Control*, pages 951–959, 1994.

C. W. Scherer. Multiobjective $\mathcal{H}_2/\mathcal{H}_\infty$ Control. *IEEE Transactions on Automatic Control*, pages 1054–1062, 1995.

C. Sonntag. Control-relevant Identification of a Reactive Distillation Column. Dipl.-Ing. Thesis, Universität Dortmund, Dortmund, May 2004.

M. Sznaier, H. Rotstein, J. Bu, and A. Sideris. An Exact Solution to Continuous-time Mixed $\mathcal{H}_2/\mathcal{H}_\infty$ Control Problems. *IEEE Transactions on Automatic Control*, pages 2095–2101, 2000.

A. F. Tulleken, Herbert J. Generalized Binary Noise Test-signal Concept for Improved Identification-experiment Design. *Automatica*, pages 37–49, 1990.

P. M. J. Van Den Hof, P. S. C. Heuberger, and J. Bokor. System Identification with Generalized Orthonormal Basis Functions. *Automatica*, pages 1821–1834, 1995.

M. Völker. Robuste, Lineare Regelung einer Reaktiven Rektifikationskolonne (Robust, Linear Control of a Reactive Distillation Column). Dipl.-Ing. thesis, Universität Dortmund, 2002.

M. Völker and S. Engell. Quantitative I/O-Controllability Assessment for Uncertain Plants. In *Proceedings of the Conference on Computer-aided Control System Design*, pages 13–18, Taipei, Taiwan, 2004. IEEE.

M. Völker and S. Engell. Multiobjective Controllability Assessment by Finite Dimensional Approximation. In *Accepted for: 24th American Control Conference*, Portland, Oregon, 2005.

K. Webers. *Bestimmung der erreichbaren Regelgüte durch konvexe Optimierung (Calculation of the Achievable Control Performance by Convex Optimization)*. Dr.-Ing. Dissertation, Universität Dortmund, 1997a. Shaker Verlag, Aachen.

K. Webers. Controller Design via LMI-based Stability Test and Convex Optimization. In *2nd IFAC Symposium on Robust Control Design*, pages 223–228, 1997b.

K. Webers and S. Engell. Comparison of Multivariable and Decentralised Control for a CSTR by Convex Optimisation. In *13th IFAC World Congress*, pages 391–396. IFAC, 1996a.

K. Webers and S. Engell. Controller Structure Evaluation by Convex Optimization. *Computers and Chemical Engineering*, pages 949–954, 1996b.

D. Youla, H. Jabr, and J. Bongiorno. Modern Wiener-Hopf Design of Optimal Controllers-Part II: The Multivariable Case. *IEEE Transactions on Automatic Control*, pages 319–338, 1976.

K. Zhou. *Essentials of Robust Control*. Prentice Hall, 1998.

Y. C. Zhu. Black-box Identification of MIMO Transfer Functions: Asymptotic Properties of Prediction Error Models. *International Journal of Adaptive Control and Signal Processing*, pages 357–373, 1989.

Y. C. Zhu. *Multivariable System Identification for Process Control*. Pergamon, Amsterdam, London, New York, Oxford, Paris, Shannon, Tokyo, 2001. ISBN 008 043985-3.